Preparation of flower-like MgO *via* spray drying with high adsorption performance

Mengjie Kuang[1], Gaoling Yang[1], Zeming Xie[1], Qi Su[1], and Baixiong Liu[2,*]

[1] School of Materials Science and Engineering, Jiangxi University of Science and Technology, Jiangxi, Ganzhou 341000

[2] Engineering Research Center of High-efficiency Development and Application Technology of Tungsten Resources, Jiangxi University of Science and Technology, Jiangxi, Ganzhou 341000

[*] Corresponding author. Tel/Fax: +86-797-8312705. E-mail: liu_micro@126.com

Abstract: Flower-like MgO was synthesized by spray drying combined with heat treatment. The morphologies of MgO can be controlled by adjusting calcination temperature. The adsorption properties of MgO powder as adsorbent to Congo red were studied. When calcination temperature was 350ºC, a flower-like MgO nanostructure with a high BET surface area of 180.5$m^2.g^{-1}$was obtained, and the saturated adsorption capacity of Congo red solution was about 2140$mg.g^{-1}$. Furthermore, the adsorption model was explored, and the result shows that the adsorption process accords with Langmuir adsorption model. The high uptake capability of the as-prepared flower-like MgO makes it as a potentially attractive adsorbent for the removal of organic dyes from water.

1. Introduction

Water is vital to human beings and other creatures. However, with the rapid development of industry and long-term sewage discharge, water has been seriously polluted [1, 2]. Organic dyes and heavy metal ions, which are seriously damaged to the ecological environment and endangered to people's health, are two important sources of pollutions. Among organic dyes, Congo red is one of typical pollutants in printing and dyeing industry. It has a structure with benzene ring, azobenzene and biphenyl, resulting strong toxicity. Moreover, it will form carcinogenic substances in the action of azo reduction, which will bring great potential threat to human beings and aquatic organisms. Therefore, the removal of Congo red from water is of great significance for environmental protection. At present, how to effectively remove pollutants from water has become a hot spot of research [3, 4]. Many methods, including electrochemistry, photodegradation, biodegradation, adsorption and so on, have been reported to use to treat Congo red sewage [5, 6]. In these methods, adsorption is widely used because of its high efficiency, large adsorption capacity, easy operation and low cost [7]. However, the traditional adsorbents have many problems, such as limited adsorption properties, poor adsorption selectivity and not easy to regenerate, which are not conducive to the widespread use of the adsorbents. In recent years, adsorbents with nanostructures have provided an important direction for solving water treatment problems because of their high surface area, good electrostatic mechanism, and rich active reaction sites [8]. It is considered that they can effectively remove inorganic and organic pollutants in sewage [9]. Liu et al. prepared the composite nanowires of graphene oxide and $Mg(OH)_2$. The saturated adsorption capacity of the Congo red solution was only 118$mg.g^{-1}$. The maximum adsorption

capacity of the porous CeO_2 nanotubes prepared by Wu et al. [10] was 362.32mg.g^{-1}. The adsorption performance of Congo red on these materials are a little bit low and the preparation processes are complex. Therefore, it is urgent to find more efficient materials with high surface area, porous structure, low cost and easy preparation.

Nanostructured MgO as an adsorbent not only has the characteristics of traditional MgO materials, but also has high specific surface area, abundant reaction sites, ideal mechanical strength, etc. Thus, it has a good application prospect in wastewater treatment [11]. At present, the methods of preparing nanostructured MgO include sol-gel, hydrothermal, flame spray pyrolysis, laser vaporization, chemical vapor deposition, combustion aerosol synthesis, surfactant and so on [12], among which hydrothermal method has been reported is the most. However, the reported preparation processes are complicated and inefficient [13]. Spray drying is an established method that is initiated by atomizing suspensions into droplets followed by a drying process, resulting in solid particles [14]. It is widely used to prepare powders because of its many advantages, including a simple system, high efficiency, low preparation temperature and the fact that it can be scaled up to ton quantities. In this paper, $Mg(CH_3COO)_2$ precursor was prepared by spray drying, and then combined with heat treatment process to prepare MgO nano-adsorption material. The prepared nano-MgO exhibits good adsorption performance for Congo red dye in aqueous solution and has a good application prospect for sewage purification.

2. Experiment

2.1 Chemicals

Magnesium acetate ($Mg(CH_3COO)_2{\cdot}4H_2O$), Congo red and ethanol were purchased from Beijing Chemical Corp. All chemicals were analytically pure and used as received without any further purification.

2.2 Preparation of materials

2.2.1. Synthesis of flower-like nano MgO powder. Nano MgO adsorption materials were synthesized by spray drying method. At first, magnesium acetate was dissolved in deionized water to form solution with a concentration of 40g·L^{-1}, and then $Mg(CH_3COO)_2$ hollow spheres were prepared by spray drying using YC-015 spray dryer under the fan speed of 60r·min^{-1}, feeding speed of 300mL/h. And inlet temperature, outlet temperatures are 230ºC and 110ºC, respectively. Subsequently, calcination was conducted in SK-G08143 high-temperature tube oven at 350ºC for 60min with heating rate of 5ºC/min and the specimen was cooled to room temperature naturally.

2.2.2. Adsorption test. 0.02g MgO was added into 0.02L of Congo red solution at different concentrations (100mg·g^{-1} to 2500mg·l^{-1}). After stirring at room temperature for 12h, the supernatant was centrifuged. The absorption spectrum was monitored by an UV-visible spectrophotometer (Shimadzu, UV-3600 plus), and the equilibrium concentration (C_e) of the adsorbate in the solution was calculated from the ratio of the corresponding absorbance to the absorbance of the standard solution. The corresponding equilibrium adsorption amount (q_e) can be calculated according the formula as follows:

$$q_e = (C_o - C_e)V/m$$

wherein C_o represents initial concentration, V is solution volume and m is the quality of adsorbent. The fitting was performed by Langmuir adsorption model to calculate the saturated adsorption capacity.

2.3. Characterization

Thermal behaviour of $Mg(CH_3COO)_2{\cdot}4H_2O$ was carried out by differential thermal analysis (DTA) and thermo gravimetric analysis (TG) (TG/DTA 6300, Perkin Elmer). The phase of the prepared powder was measured by X-ray diffractometer (XRD, Rigaku D-max 2500).The surface morphology was characterized with a Hitachi S-4800 scanning electron microscope. The Brunauer–Emmett–Teller

(BET) method was utilized to calculate the specific surface areas. The pore size distributions were derived from the adsorption branches of the isotherms based on the Barrett–Joyner–Halanda (BJH) model.

3. Results and discussion

Figure 1 shows the TG-DTA curves for $Mg(CH_3COO)_2 \cdot 4H_2O$ sample calcined under flowing air from room temperature to 1000°C at a rate of 5°C·min^{-1}. The TG curve gradually decreases with increasing temperature. In the TG analysis, two main mass-loss stages are observed. The first mass loss occurs in the range of 60 ~ 172.9°C. This weight loss, which is ~ 33.5%, can be attributed to the removal of crystalline water from $Mg(CH_3COO)_2 \cdot 4H_2O$. In the second stage, the weight loss is ~ 42.5%, which is take place in the range 319°C ~ 400°C. Practically, no mass loss was observed above 600°C. The reactions are as following:

$$Mg(CH_3COO)_2 \cdot 4H_2O = Mg(CH_3COO)_2 + 4H_2O \ (\Delta_m = 33.7\%) \quad (1)$$

$$Mg(CH_3COO)_2 + 4O_2 = MgO + 3H_2O + 4CO_2 \quad (\Delta_m = 47.6\%) \quad (2)$$

There is an endothermic peak at ~ 82.6°C and an exothermic peak at ~ 328.8°C, which correspond to evaporation of crystal water and decomposition of $Mg(CH_3COO)_2$, respectively. The heat treatment temperature of the precursor is the key factor to synthesize spherical-like MgO. If the temperature is too low, $Mg(CH_3COO)_2$ would be incomplete decomposition. Therefore, on the basis of ensuring $Mg(CH_3COO)_2$ to be completely decomposed, calcination temperature for $Mg(CH_3COO)_2$ should be set up to 328.8°C.

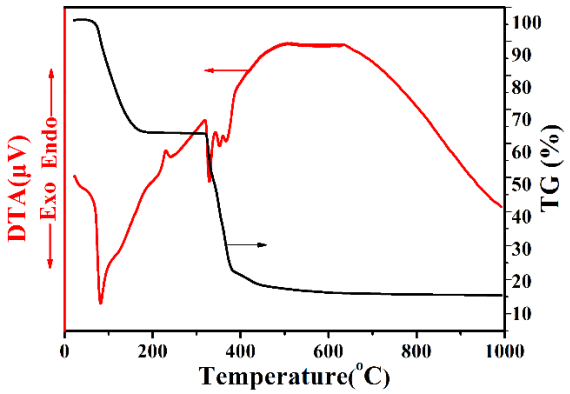

Figure 1. TG and DTA curves of $Mg(CH_3COO)_2 \cdot 4H_2O$ sample.

Figure 2 shows the XRD pattern of the sample. It can be seen that the product obtained by calcining the precursor at 350°C has a small amount of impurities in addition to MgO. This is due to the fact that the lower temperature during the heat treatment and the excessive heating rate, which results the incomplete decomposition of the precursor. Compared with the standard XRD pattern, the prepared sample has a face-centered cubic crystal structure. The XRD peak of the sample is a broad peak with low intensity, which is characteristic of typical nanoparticles.

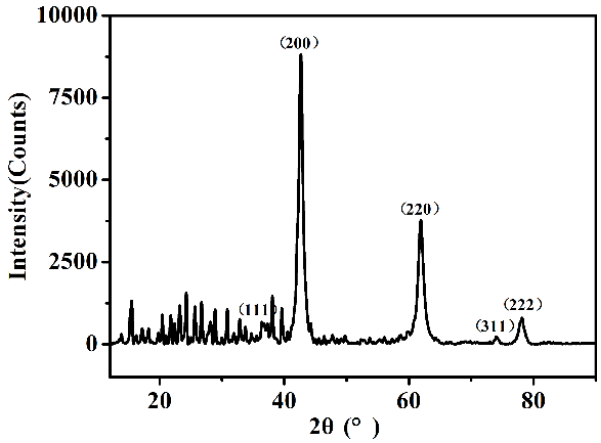

Figure 2. XRD patterns for sample treated at 350°C.

Figure 3a shows SEM image of as-synthesized powder. It can be clearly observed that the flower-like morphology was formed by the twisted nanosheets and the architectures approximately 1μm in diameter. The detailed morphology of the flower-like nanostructures is shown in Figure 3b, which reveals that the entire structure of the architecture is built from several dozen nanosheets with smooth surfaces. These nanosheets were ca. 0.1μm thick and connected to each other through the center to form 3D flower like structures.

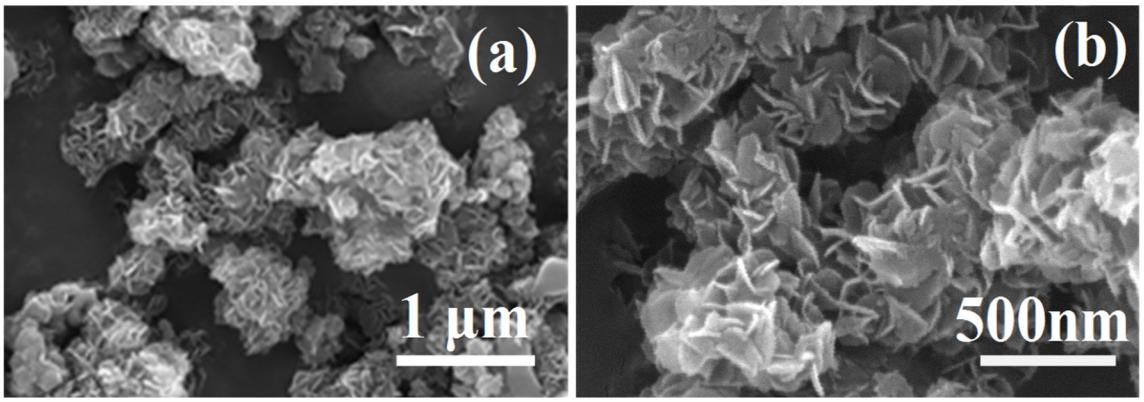

Figure 3. SEM images for sample treated at 350°C.

Figure 4 shows the N_2 adsorption-desorption isotherm and the corresponding pore-size distribution of the MgO sample. It can be seen that the isotherm shows representative type-IV curve with H_4 hysteresis loop. Obvious capillary condensation is observed at a relative pressure (P/P_0) of 0.45-0.8. The pore-size distribution curve calculated from the adsorption branches confirms a narrow pore size distribution. It indicates that the pore size distribution of as-prepared sample is within the range of mesopores. The calculated specific surface area is 180.5m^2/g and average pore size is 7nm.

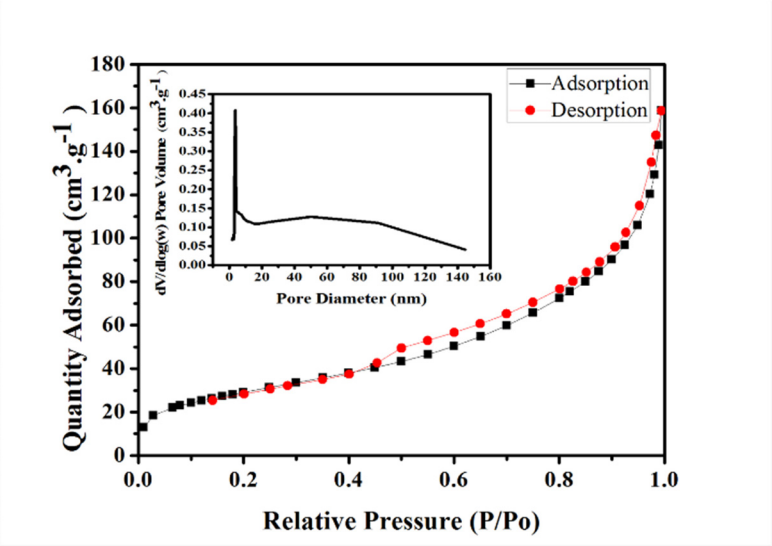

Figure 4. N_2 adsorption–desorption isotherms of the MgO sample and pore size distribution.

The prepared nano-powder is applied to sewage purification. In this paper, Congo red solution was used as simulated wastewater. The adsorption performance of the sample was characterized by testing its isothermal adsorption and adsorption rate of Congo red solution. Langmuir adsorption model was used to study the relationship between the equilibrium concentration of adsorbates and the amount of adsorbent adsorbed in solution at constant temperature. The formula of Langmuir model is as follows:

$$q_e = q_m b C_e / (1 + K_L C_e)$$

wherein b represents equilibrium constant, q_e, C_e and q_m represent balanced adsorption capacity, balanced solution adsorbate concentration and maximum adsorption capacity, respectively.

The Langmuir isotherm model was used to fit the experimental data. Figure 5 shows that it is a homogeneous monolayer adsorption process. The saturated adsorption amount of the Congo red solution calculated is 2140mg.g^{-1}.

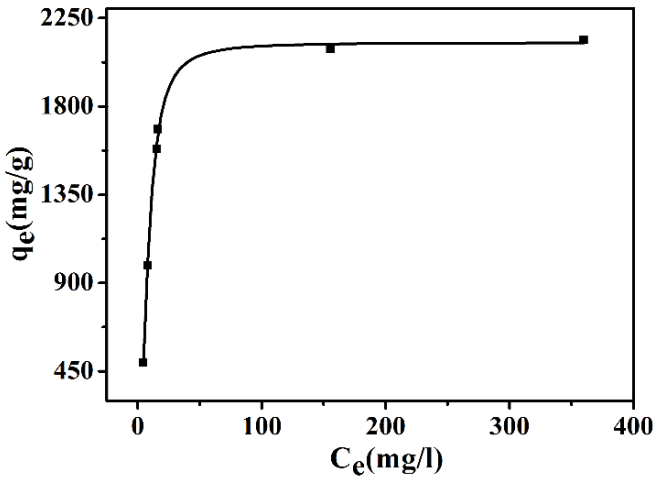

Figure 5. Langmuir model fitting curve of nano-MgO as adsorbent for Congo red dye adsorption.

4. Conclusions

XRD and SEM analysis showed that spray drying combined with heat treatment can efficiently produce powder with surface morphology of petal. The flower-like MgO was obtained when calcination was 350ºC which had good adsorption performance. The specific surface area was

180.5m^2/g. The saturated adsorption capacity of Congo red solution was 2140mg.g^{-1}. The adsorption data of the prepared flower-like MgO on the Congo red solution satisfies the Langmuir isothermal adsorption model, indicating that the adsorption process is a homogeneous monolayer adsorption process.

Acknowledgment
This work was supported by National Natural Science Foundation of China (grant number 51664023) and Natural Science Foundation of Jiangxi Province (20161BAB206144, GJJ150688).

References:
[1] Fujishima A, Honda K. Photolysis-decomposition of water at surface of an irradiated semiconductor[J]. *Nature*, 1972, **238**(1):238-245.
[2] Cai Y, Li C, Wu D, et al. Highly active MgO nanoparticles for simultaneous bacterial inactivation and heavy metal removal from aqueous solution[J]. *Chemical Engineering Journal*. 2017, **312**: 158-166.
[3] Qu X, Alvarez P J, Li Q. Applications of nanotechnology in water and wastewater treatment[J]. *Water Research*. 2013, **47**(12): 3931-3946.
[4] Jia Y, Luo T, Yu X Y, et al. A facile template free solution approach for the synthesis of dypingite nanowires and subsequent decomposition to nanoporous MgO nanowires with excellent arsenate adsorption properties[J]. *Royal Society of Chemistry Advances*. 2013, **16**(3): 5430-5437.
[5] Li X, Xiao W, He G, et al. Pore size and surface area control of MgO nanostructures using a surfactant-templated hydrothermal process: High adsorption capability to azo dyes[J]. *Colloids & Surfaces A Physicochemical & Engineering Aspects*. 2012, **408**(16): 79-86.
[6] Wang Y, Wang G, Wang H, et al. Chemical-template synthesis of micro/nanoscale magnesium silicate hollow spheres for waste-water treatment.[J]. *Chemistry-A European Journal*. 2010, **16**(11): 3497-3503.
[7] Cheng K, Hu J, Hou H, et al. Aerobic granular sludge inoculated microbial fuel cells for enhanced epoxy reactive diluent wastewater treatment[J]. *Bioresource Technology*. 2017, **229**: 126.
[8] Tian Y, Li H, Ruan Z, et al. Synthesis of NiCo2O4 nanostructures with different morphologies for the removal of methyl orange[J]. *Applied Surface Science*. 2017, **393**: 434-440.
[9] Wang Q G, Sun H J, Peng T J,et al. Influence of oxidation degree of graphene oxide on adsorption performance for methylene blue[J]. *CIESC Journal*. 2017, **68**(4):1712-1720.
[10] Wu J, Wang J, Du Y, et al. Adsorption mechanism and kinetics of azo dye chemicals on oxide nanotubes: a case study using porous CeO_2 nanotubes[J]. *Journal of Nanoparticle Research*. 2016, **18**(7):191.
[11] Mohamed R M, Shawky A, Mkhalid I A. Facile synthesis of MgO and Ni-MgO nanostructures with enhanced adsorption of methyl blue dye[J]. *Journal of Physics & Chemistry of Solids*. 2017, **101**: 50-57.
[12] Hanlon J M, Diaz L B, Balducci G, et al. Rapid surfactant-free synthesis of $Mg(OH)_2$ nanoplates and pseudomorphic dehydration to MgO[J]. *Crystengcomm*. 2015, **17**(30): 5672-5679.
[13] Cao C, Qu J, Wei F, et al. Superb Adsorption Capacity and Mechanism of Flowerlike Magnesium Oxide Nanostructures for Lead and Cadmium Ions[J]. *Accounts of Chemical Research Applied Materials & Interfaces*. 2012, **4**(8): 4283-4287.
[14] Waldron K, Wu Z, Wu W D, et al. Formation of uniform large SBA-15 microspheres via spray drying[J]. *Journal of materials chemistry* A. 2014, **2**(45): 19500-19508.